MATERIALS SCIENCE

Torsional refrigeration by twisted, coiled, and supercoiled fibers

Run Wang[1]*, Shaoli Fang[2]*, Yicheng Xiao[1], Enlai Gao[2,3], Nan Jiang[2,4], Yaowang Li[5], Linlin Mou[1], Yanan Shen[1], Wubin Zhao[1], Sitong Li[1], Alexandre F. Fonseca[6], Douglas S. Galvão[6], Mengmeng Chen[1], Wenqian He[1], Kaiqing Yu[1], Hongbing Lu[7], Xuemin Wang[7,8], Dong Qian[7], Ali E. Aliev[2], Na Li[2,9], Carter S. Haines[2], Zhongsheng Liu[1], Jiuke Mu[2], Zhong Wang[2], Shougen Yin[10], Márcio D. Lima[11], Baigang An[12], Xiang Zhou[13], Zunfeng Liu[1]†, Ray H. Baughman[2]†

Higher-efficiency, lower-cost refrigeration is needed for both large- and small-scale cooling. Refrigerators using entropy changes during cycles of stretching or hydrostatic compression of a solid are possible alternatives to the vapor-compression fridges found in homes. We show that high cooling results from twist changes for twisted, coiled, or supercoiled fibers, including those of natural rubber, nickel titanium, and polyethylene fishing line. Using opposite chiralities of twist and coiling produces supercoiled natural rubber fibers and coiled fishing line fibers that cool when stretched. A demonstrated twist-based device for cooling flowing water provides high cooling energy and device efficiency. Mechanical calculations describe the axial and spring-index dependencies of twist-enhanced cooling and its origin in a phase transformation for polyethylene fibers.

Compared with conventional vapor-compression refrigerators, a solid that changes entropy when deformed could possibly provide higher efficiency; lower cost, weight, and volume; and more convenient miniaturization. An ordinary rubber band is an example, which was reported in 1805 to heat when stretched and to cool when stretch is released (1). Alternative materials for refrigeration are electrocaloric (2–6) and magnetocaloric (6, 7), meaning they provide cooling because of changes in electric or magnetic fields, respectively. Although these solid-state cooling mechanisms have been widely investigated for diverse materials, none yet meets the performance needs for wide-scale applications. In fact, thermoelectrics are the only solid-state coolers that have been commercialized, and these coolers are expensive and have low energy conversion efficiencies.

Efficiencies of ~60% of the Carnot efficiency can be obtained for vapor-compression refrigerators (8, 9), which is a mature technology that typically uses gases whose release can powerfully contribute to global warming. No alternative technology presently achieves this same efficiency. On the other hand, theoretical efficiencies of ~84% of the Carnot efficiency have been predicted for tensile deformation cycles of a NiTi shape memory alloy (9). Realization of close to this efficiency could have enormous consequences if the needed cycle

life of vapor-compression refrigerators could be obtained, given that so much of global energy consumption goes to cooling.

Refrigeration materials that undergo cooling because of any type of mechanical deformation are called mechanocaloric, and those that cool because of changes in uniaxial stress (5, 6, 9–15) or hydrostatic pressure (6, 15–17) are more specifically called elastocaloric and barocaloric, respectively (6). In this study, we demonstrate cooling by a change in yarn or fiber twist, which we call twistocaloric cooling. We call coolers that use twist changes for refrigeration "twist fridges."

Twist-based cooling using single natural rubber fibers

Vulcanized natural rubber (NR) fibers (18) (figs. S1 to S10) provide a prototypical twistocaloric material. Twisting these fibers causes coil nucleation and propagation, decreasing intercoil separation, and ultimately nucleation of supercoils (Fig. 1A). For isometric strains (i.e., constant strains during twist) of 100, 250, 300, and 450%, fracture occurs before completion of supercoiling, initiation of supercoiling, completion of coiling, and initiation of coiling, respectively. Unless otherwise stated, (i) stresses, strains, and twist densities are relative to the cross-sectional area or length of the non-deformed fiber (called the parent fiber), and (ii) a tensile strain rate of 42 cm/s and a twist-

ing and untwisting rate of 50 turns/s were used for NR fibers having a nondeformed length of 3.0 cm. Here and elsewhere, tensile strain changes are made either while a fiber or yarn is torsionally tethered or for the nontwisted state.

Twistocaloric surface temperature changes occur inhomogeneously for coiled and supercoiled fibers. Hence, maximum and average surface temperature changes (ΔT_{max} and ΔT_{avg}, respectively) are reported. Surface temperatures were measured using a thermal camera, whose accuracy was established by comparison with thermocouple measurements in a temperature-controlled oven on fibers with different twist states (18).

The temperature swing on stretch and stretch release (between heating and cooling temperatures) is important for remotely optically readable strain sensors or mechanothermochromic fibers. For 300% isometric strain, this swing in surface-average temperature was 3.3°, 6.5°, and 7.7°C for highly twisted, coiled, and partially supercoiled fibers, respectively, compared with 2.4°C for a nontwisted fiber (Fig. 1B). The maximum surface temperature swing (fig. S11B) for this modest applied strain was 5.4°, 10.5°, and 12.9°C for the highly twisted, coiled, and partially supercoiled fibers, which is up to 5.4 times that for the nontwisted NR fiber. However, when released from strains >300%, nontwisted NR fibers provided greater surface cooling. Hence, these twisted NR fibers are not very useful for refrigerators that solely use large-magnitude stretch and release.

Examples of cooling by untwist are shown in Fig. 1, C to E; figs. S13 to S18; and movie S1. When twist is released from a supercoiled NR fiber having 100% isometric strain, the maximum (−15.5°C) and average (−12.4°C) surface cooling exceed that for 600% stretch release from a nontwisted fiber (−12.2°C) (Fig. 1B). By releasing twist and then stretch (Fig. 2, A and B), even higher maximum (−16.4°C) and average (−14.5°C) cooling was obtained. Hence, a twist-based cooler at 100% strain can be two-sevenths of the maximum length of the above stretch-based cooler and still provide 2.3°C higher surface-average cooling. Figure S34A and movie S2 illustrate the use of a thermochromic dye–coated NR fiber as a mechanothermochromic material whose color responds to changes in inserted twist.

The heating and cooling during stretch and stretch release of a nontwisted fiber are

approximately independent of fiber diameter (fig. S11A). Also, NR fibers having different diameters but the same elongation have approximately the same dependence of ΔT_{max} and ΔT_{avg} on the product of twist density and stretched fiber diameter (fig. S17). The maximum surface cooling on twist release was essentially the same whether twist insertion was done isometrically (for constant tensile strain) or isobarically (for constant tensile load), as long as the percent stretch obtained after isometric twist release was identical (fig. S19). The NR fiber showed stable heating and cooling during isometric twisting and untwisting up to 15 turns/cm for 750 cycles (fig. S21).

Volume-average cooling for twisted NR fibers

The volume-average cooling upon untwisting a NR fiber was obtained from the cooling energy of this fiber in a water-containing plastic tube (fig. S44A). This cooling energy is the sum of the products of gravimetric heat capacity, mass, and temperature decrease for the water, plastic tube, and NR fiber after internal thermal equilibration of the system (fig. S44B). The volume-average cooling upon untwisting a NR fiber was obtained by dividing the derived cooling energy by the heat capacity and mass of the NR fiber (18). To minimize loss of cooling energy to surrounding air (fig. S12) by decreasing the temperature change of the water, a mass of water 4.63 times that of the NR fiber was used. This small loss of cooling energy was corrected by fitting the long-term temperature dependence of water and container to a standard heat-loss equation (19) and then adding these temperature corrections to the observed curves, so that the loss-corrected temperature curves reach long plateaus (18). The temperature changes for these plateaus were used to obtain the cooling energy and thereby the dependence of volume-average temperature change on twist density change.

Figure 1D compares the surface-average and volume-average temperature changes for isometric twist insertion and release from a 100% stretched NR fiber. For the high twist density most important for applications, where the twist removal time (1.5 s) exceeds the calculated radial thermal equilibration time (0.96 s) (18), the volume-average cooling is 11.3°C and the ratio of volume-average to surface-average temperatures reaches 0.91. This is consistent with nearly complete equilibration in the radial direction.

Although the maximum twistocaloric specific cooling energy obtained (19.4 J/g) is lower than reported for releasing 600% stretch from a nontwisted NR fiber (21.6 J/g) (20), the stretch needed for this torsional cooling is much smaller (100%). At 100% strain, stretch-based cooling would only be 4.2% of that delivered by twistocaloric cooling (18).

Coefficients of performance for twisted NR fibers

Using the above volume-average cooling on isometric twist release, the coefficient of performance (COP) for NR twist fridges was obtained. The COP can be described as the ratio of the cooling energy (the product of the volume-average cooling, the gravimetric heat capacity, and the mass of the fiber) to either the input mechanical energy or the net energy consumed during a mechanical cycle (called

COP_{HC} and COP_{FC}, for a half cycle and a full cycle, respectively) (6). COP_{HC} is useful when device simplicity or miniaturization is more important than increasing efficiency by recapturing part of the input mechanical energy.

Using the stretch release–induced cooling of the nontwisted fiber (Fig. 1B), the volume-average cooling during twist release (Fig. 1D), and mechanical measurements (figs. S7 and S10B), the COPs were obtained as a function of volume-average cooling (Fig. 2C and fig.
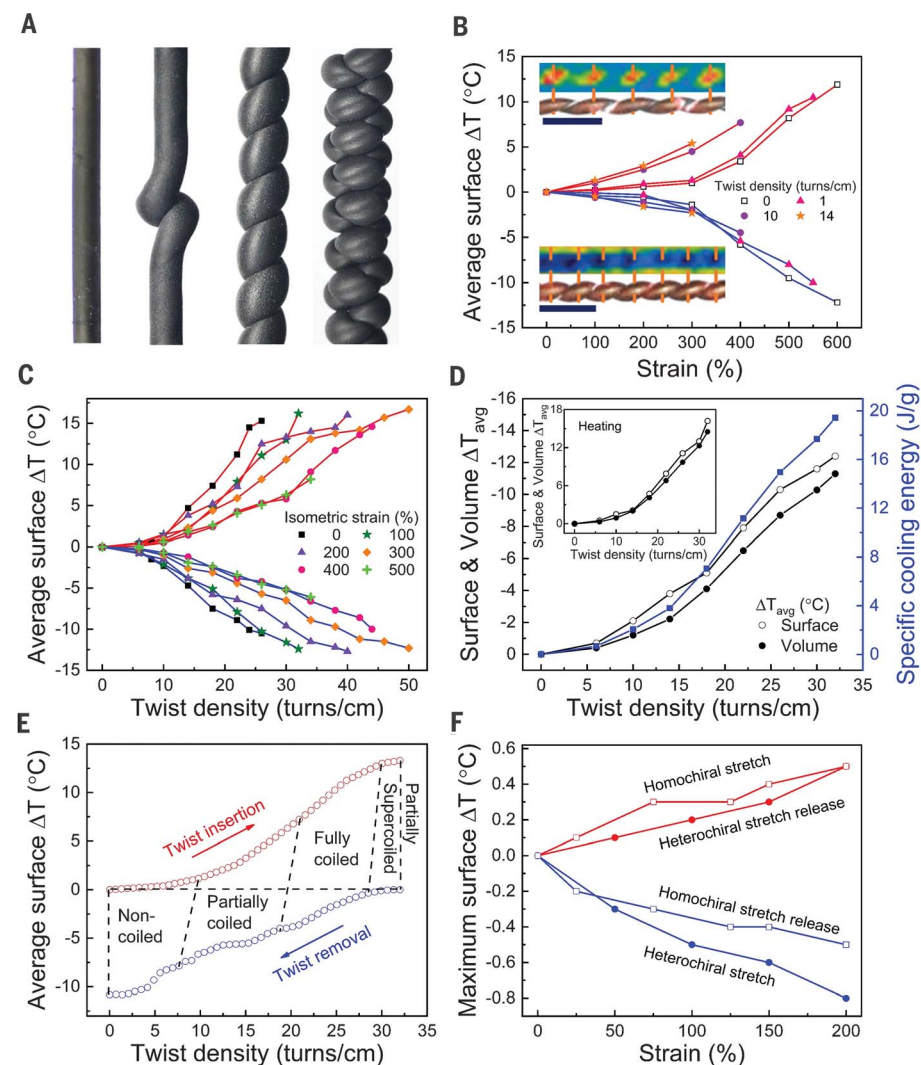

Fig. 1. Twist-based mechanocaloric performance for single rubber fibers. (**A**) Photographs of twisted, partially coiled, fully coiled, and fully supercoiled 2.5-mm-diameter NR fibers at 100% strain. The background was digitally removed. (**B**) Surface-average temperature changes versus strain for NR fibers having 0, 1, 10, and 14 turns/cm of twist (nontwisted, highly twisted, fully coiled, and partially supercoiled, respectively, in the nonstretched state). Insets show thermal and optical photographs after 100% stretch (top) and after stretch release (bottom) for a coiled NR fiber (18 turns/cm). Scale bars: 0.5 mm. (**C**) Surface-average temperature changes of a NR fiber during isometric twist and untwist at different tensile strains. (**D**) Surface-average cooling, volume-average cooling, and specific cooling energy for isometrically untwisting a NR fiber at 100% strain. Inset shows corresponding results for volume-average and surface-average heating. (**E**) Surface-average temperature changes for isometrically twisting and untwisting a NR fiber at 200% strain, when measured continuously during an increasing twist and a decreasing twist scan. (**F**) Twistocaloric temperature changes versus strain for heterochiral and homochiral coiled NR fibers. In the experiments corresponding to (B) to (F), 2.2-mm-diameter NR fibers were used.

S43). The COP$_{FC}$ and COP$_{HC}$ for cooling, either by twist release or by releasing twist and then stretch, are much higher than for cooling by stretch release from the nontwisted fiber when the volume-average cooling is above −0.4°C (Fig. 2C and fig. S43). For the highest volume-average cooling obtained for releasing stretch from a nontwisted fiber (−12.2°C), isometric untwist (−11.3°C), and releasing twist and then stretch (−12.1°C), the COP$_{FC}$ values are 3.8, 8.3, and 8.5, respectively (Fig. 2C), and the COP$_{HC}$ values are 1.9, 5.2, and 5.3, respectively (fig. S43).

The intrinsic efficiency of a material, which is the maximum theoretical efficiency for a refrigerator, is the ratio of COP$_{FC}$ to the COP of a Carnot cycle (COP$_{Carnot}$). COP$_{Carnot}$ is $T_C/(T_H - T_C)$, where T_C and T_H are the minimum and the maximum temperatures in the cycle, respectively. These material efficiencies for cooling during isometric untwisting and during releasing twist and then stretch are much higher than for cooling during stretch release from a nontwisted fiber, for both full-cycle and half-cycle processes (fig. S43, C and D). For the highest volume-average cooling for

stretch release from a nontwisted fiber, isometric untwisting, and releasing twist and then stretch, the full-cycle intrinsic material efficiencies were 0.32, 0.63, and 0.67, respectively.

Twist-based cooling by plying NR fibers

To demonstrate scalability, cooling was measured while isometrically unplying multiple NR fibers. Unplying seven-ply 2.2-mm-diameter NR fibers (Fig. 2, D and E) produced higher maximum (−19.1°C) and average (−14.4°C) surface cooling than for 600% stretch release from a nontwisted fiber (−12.2°C) (Fig. 1B) or for isometric untwisting of a 100% stretched single fiber (−15.5°C maximum and −12.4°C average) (Fig. 1C and fig. S15). Unplying from isometric strains around 100% produced the highest twistocaloric cooling (figs. S23 and S24).

Guided by the correspondence between twistocaloric cooling for single fibers having the same stretch, and a similar product of twist density and stretched fiber diameter (fig. S17), we found that the twistocaloric cooling associated with isometric fiber plying approximately depends on the product of the twist density of plying and the effective diameter of the bundle ($D_{eff} = n^{0.5} \times D_s$, where n is the number of fibers and D_s is the stretched fiber diameter) (Fig. 2E).

Spatial and temporal dependencies of twistocaloric temperature changes for NR fibers

Spatially complex surface temperature changes occur for twistocaloric processes for coiled or supercoiled fibers (Fig. 2F and fig. S20). Like for a bent cantilever, the inside of a coiled fiber is compressed and the outside is stretched, causing the coil's exterior to undergo the highest temperature change during coil formation and removal. Painting the exterior of a coiled fiber enabled demonstration that these maximum strained regions have the highest cooling after fiber untwisting. The periodicity of these regions on the surface of the untwisted fiber (5.6 mm) is much longer than the average coil period of the fully coiled fiber (2.5 mm).

The peak surface cooling increases with increasing distance from the site where coiling nucleates (fig. S20), because coiling stretches noncoiled fiber regions and thereby decreases the spring index (the ratio of the average coil diameter to the diameter of the fiber within the coil) of later-introduced coils. The sharp change in maximum surface cooling upon complete removal of coiling (fig. S17A) disappears when measuring average cooling (fig. S17B), indicating that the effects of bending approximately average to zero. Because the number of coils is strain invariant, the separations between temperature peaks during both stretching and releasing are identical to the intercoil separations (Fig. 1B, inset).
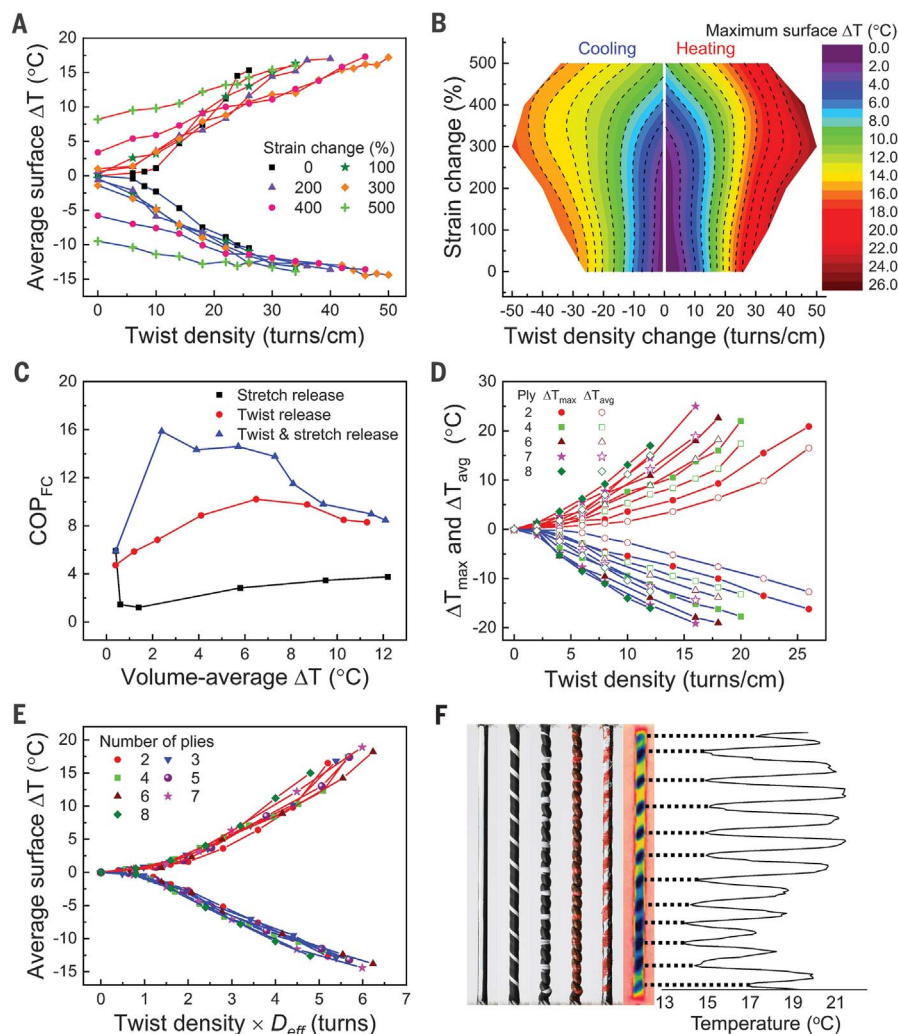

Fig. 2. Mechanocaloric performance of single and plied NR fibers during twist and stretch.
(**A**) Average and (**B**) maximum surface temperature changes of a NR fiber during sequential stretch and then isometric twisting and during sequential isometric untwisting and then stretch release. (**C**) The COP$_{FC}$ versus volume-average cooling for releasing up to 600% strain from a nontwisted fiber (black), isometric untwisting a fiber at 100% strain (red), and isometric untwisting at 100% strain followed by stretch release (blue). (**D**) The maximum and surface-average temperature changes versus twist density for plying and unplying NR fibers at 100% strain. (**E**) The surface-average temperature changes of (D) versus the product of twist density and the effective fiber diameter. In the experiments corresponding to (A) to (E), 2.2-mm-diameter NR fibers were used. (**F**) Photographs of an initially nontwisted, 3-cm-long, 3-mm-diameter NR fiber that was (from left to right) stretched to 100% and painted with a white line along its length; highly twisted; fully coiled; painted red on the coil's exterior; and then fully untwisted. The thermal image and temperature profile (right) show the fiber immediately after removing 12 turns/cm of inserted twist.

Twistocaloric cooling by self-coiled polyethylene and nylon fibers

Twistocaloric cooling was also investigated for polymers used for fishing line and sewing thread. These polymers were made elastically deformable by isobarically twisting until the fiber coils, as is done to make powerful thermally driven artificial muscles (21). These self-coiled fibers are called homochiral because fiber twist and coiling have the same handedness.

Initial experiments used 0.41-mm-diameter, 65-pound test, braided polyethylene (PE) fishing line (fig. S25A). Spring indices from 1.4 to 0.5 were obtained by inserting 6.5 to 7.3 turns/cm of twist under isobaric loads of 37.1 to 74.2 MPa, respectively. When releasing 22.7% strain, maximum and average surface cooling of −5.1°C and −3.2°C, respectively, were obtained for a spring index of 0.8 (Fig. 3A and fig. S25). For comparison, the temperature change upon stretch release of nontwisted polyethylene yarn was below ±0.1°C, and the highest reported elastocaloric cooling for a nonelastomeric polymer is −2.5°C for a poly(vinylidene fluoride-trifluoroethylene-chlorotrifluoroethylene) terpolymer (15), which is a relaxor ferroelectric (2).

The highest temperature swing between maximum heating and cooling (12.9°C, for a spring index of 0.8) was obtained for 22.7% stretch and stretch release, which is a much higher per-strain change (0.57°C per percent) than for a nontwisted NR fiber (0.04°C per percent for 600% strain). This high sensitivity is useful for mechanothermochromic indicators (movie S3). No degradation in performance occurred during the investigated 2500 stretch-release cycles to 13% strain (fig. S26). The twistocaloric cooling for self-coiled, high-strength polyethylene yarn at 10°C ambient temperature is smaller than for ambient temperatures of 25° and 40°C (fig. S25). In contrast, the stretch-release–induced cooling for a nontwisted NR fiber at 10°C is higher than for either higher or lower ambient temperatures (22).

Twistocaloric cooling was also observed during stretch release for coiled, single-filament nylon 6 fishing line with parent diameters (D) of 0.2, 0.4, and 0.6 mm. To ensure the same spring index (1.0), these fibers were coiled using the same isobaric stress and the same twist number (twist density times D). These homochiral fibers, having progressively larger diameters, provided progressively increasing maximum cooling (−1.3°, −1.9°, and −2.1°C) and average cooling (−0.8°, −1.2°, and −1.8°C) upon stretch release (fig. S28).

The strain dependence of twistocaloric cooling generally increases with decreasing spring index for coiled, high-strength polyethylene yarn (fig. S25), low-strength polyethylene (fig. S27), and nylon 6 fibers (fig. S28). Similarly, for coiled polymer muscles (21), higher heating is needed to cause a given stroke for a smaller spring-index muscle. The origin in both cases is
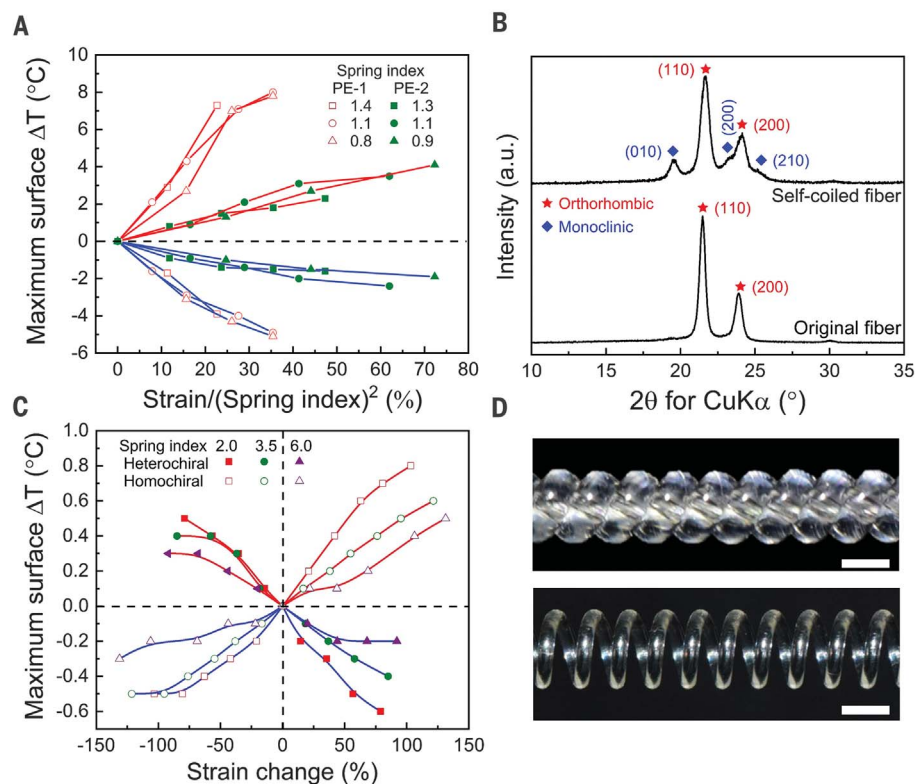
Fig. 3. Twistocaloric performance for coiled polyethylene and nylon 6. (**A**) The maximum changes in surface temperature versus the ratio of tensile strain to the square of spring index, for high-strength and low-strength polyethylene fibers (PE-1 and PE-2, respectively). (**B**) XRD for nontwisted and self-coiled PE-1 fibers. (**C**) Twistocaloric temperature changes versus strain for homochiral and heterochiral coiled nylon 6 fibers having different spring indices. (**D**) Optical images of a self-coiled, 0.6-mm-diameter nylon 6 fiber (top) and a thermally annealed (180°C for 1 hour), mandrel-coiled, 0.6-mm-diameter nylon 6 fiber (bottom). Scale bars: 1.0 mm (top) and 2.0 mm (bottom).

the stretch-induced twist change per fiber length, whose magnitude is spring-index dependent.

Theoretical results (18) (fig. S39) show that the stretch-induced twist change per fiber length, divided by the percent stretch of a coiled fiber, should approximately depend on the inverse square of spring index. This dependence arises because both the strain needed to pull out one coil and the fiber length per coil linearly increase with coil diameter. In agreement, the observed twistocaloric temperature changes for self-coiled polyethylene and nylon 6 fibers or yarns are approximately proportional to the ratio of percent stretch to the square of the spring index (Fig. 3A and fig. S40). This dependency is predicted only for the case where different-spring-index yarns have approximately the same initial coil bias angle. Owing to the difficulty of controlling this coil bias angle for later-described mandrel-coiled fibers, deviations from these theoretical results are observed.

Origin of twistocaloric cooling of polyethylene fibers

Because the above polyethylene and nylon 6 fibers are crystalline, it is challenging to ex-

plain the origin of the entropy decrease caused by stretching the coiled fiber. One possible explanation for polyethylene is the known deformation-driven orthorhombic-to-monoclinic phase conversion (fig. S41) (23–26). Using molecular dynamics calculations at 300 K (18), we predict that the entropy of the orthorhombic phase is 0.097 J K^{-1} g^{-1} higher than for the monoclinic phase, which agrees with the entropy difference calculated more than 30 years ago (26) from vibrational spectra (~0.12 J $K^{-1}g^{-1}$). Our predicted free energy difference resulting from this entropy change (29.1 J/g) and the specific heat capacity (27) of polyethylene (1.56 J $K^{-1}g^{-1}$) provides a predicted −18.7°C cooling if coil stretch caused complete conversion from the orthorhombic to monoclinic phase.

X-ray diffraction (XRD) measurements for polyethylene show that self-coiling results in partial conversion of orthorhombic to monoclinic phase. Thermally annealing the coiled yarn (120°C for 2 hours) largely reverses this transformation (Fig. 3B and fig. S42B) but barely affects twistocaloric cooling (fig. S42A). Stretching the coiled yarn to 20% strain reversibly increases the amount of monoclinic phase from 5.0 to 11.4% (table S2). Using this
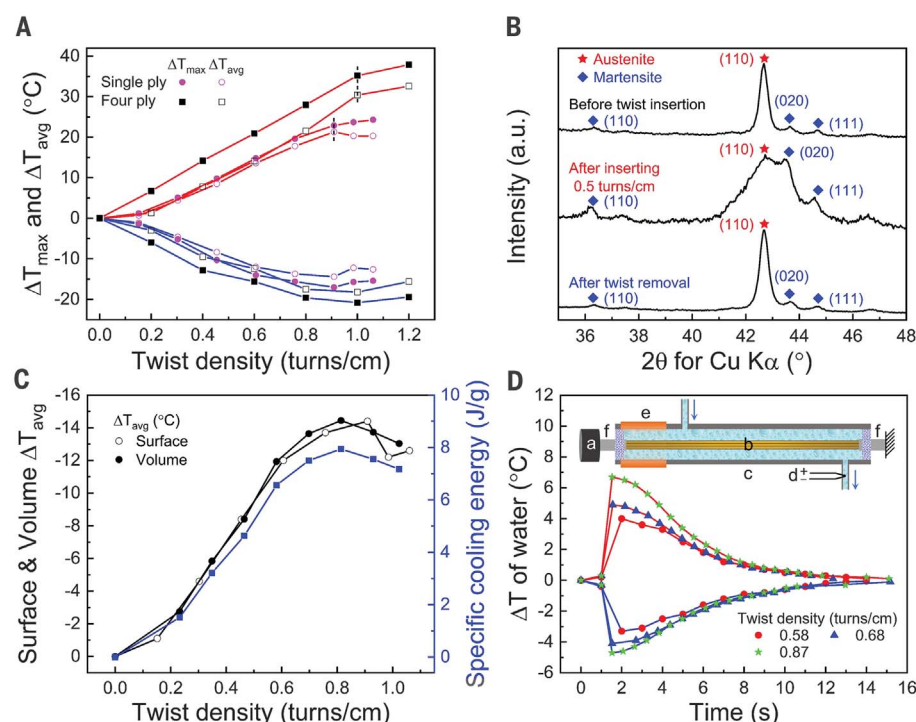
Fig. 4. Twistocaloric performance for twisted and plied NiTi wires. (**A**) The twist-induced maximum and surface-average temperature changes for a single NiTi wire and four-ply wires at 0% nominal strain. The dashed vertical lines indicate where buckling occurs. (**B**) XRD for a NiTi wire before twist insertion, after twist insertion, and after twist removal. (**C**) Surface-average cooling, volume-average cooling, and specific cooling energy for untwisting a 0.7-mm-diameter NiTi wire at 0% strain. (**D**) The time dependence of outlet water temperature change after isometric twist insertion and twist removal for a three-ply, 0.6-mm-diameter NiTi wire at a water flow rate of 0.04 ml/min using the device in the inset. This device contains (a) a motor, (b) NiTi wires, (c) a polypropylene tube containing flowing water, (d) a thermocouple, (e) a rubber tube, and (f) epoxy resin that seals the tube ends.

percent change of monoclinic phase and the −18.7°C cooling for 100% orthorhombic-to-monoclinic phase conversion, a volume-average cooling of −1.2°C is predicted for 20% strain release, which is identical to the measured surface-average cooling for this strain release. This suggests that monoclinic-to-orthorhombic phase conversion substantially contributes to twistocaloric cooling. The entropy change contribution from the amorphous phase is apparently small, which is consistent with the negligible change in amorphous scattering profile and with the unchanged ratio of the integrated diffraction intensity of the amorphous phase to the total diffraction intensity for the crystalline phases (from 0.49 to 0.50 during 20% stretch).

Twistocaloric cooling by stretching heterochiral fibers

Whereas stretch increases fiber twist for a homochiral coil, stretch causes fiber untwist for a heterochiral coil, which enables reversal of the temperature changes produced by stretch and stretch release. A heterochiral NR coil was made by wrapping a self-coiled 2.2-mm-diameter NR fiber onto a mandrel to

provide a spring index of 2.5 (18). This mandrel was retained during twistocaloric measurements to prevent twist cancellation in the rubber fiber.

This heterochiral NR coil provides an inverse mechanocaloric effect. For 200% strain, the maximum surface cooling during stretch was −0.8°C, and the maximum surface heating upon stretch release was +0.5°C (Fig. 1F and fig. S22A). For comparison, stretching and releasing the same strain from an identical spring index homochiral coil caused maximum surface temperature changes of +0.5° and −0.5°C, respectively (Fig. 1F and fig. S22B).

An inverse twistocaloric effect was also found for heterochiral coils of nylon 6 and polyethylene, which can be thermally set to maintain their coiled shape without retention of a mandrel. Stretching heterochiral coils of nylon 6 and polyethylene, with spring indices of 2.0, induces cooling of −0.6° and −0.3°C, respectively, and stretch release produces heating of +0.5° and +0.5°C, respectively (Fig. 3C and figs. S31 and S32). For comparison, stretching identical spring index homochiral coils of nylon 6 and polyethylene produces a maximum heating of +0.8° and +1.4°C, respec-

tively, and stretch release produces a maximum cooling of −0.5° and −0.6°C, respectively (Fig. 3C and figs. S29 and S30). When a heterochiral nylon 6 fiber was stretched to 90%, which is beyond the coil's yield stress, the coil irreversibly deformed to form segments having short (1.0 mm) and long (2.8 mm) intercoil periods, which cooled and heated during stretch, respectively (fig. S33).

Twistocaloric cooling by twisting and plying NiTi wires

Large, reversible temperature changes also result from twist insertion and removal from a single NiTi shape memory wire, and from plying and unplying these wires. The investigated 0.7-mm-diameter $Ni_{52.6}Ti_{47.4}$ wires had a martensite-to-austenite transition from −29.0° to 15.0°C during heating, and an austenite-to-martensite transition from 13.5° to −44.6°C during cooling (fig. S35B).

Twistocaloric cooling resulted from isometrically untwisting a single NiTi wire (−17.0°C maximum and −14.4°C average surface temperature changes) at 0% strain and at a twist rate of 50 turns/s (Fig. 4A and figs. S36 and S37). Unplying a four-ply bundle of NiTi wires produced even higher cooling (−20.8°C maximum and −18.2°C average surface temperature changes), compared with the −17.0°C elastocaloric cooling provided by an identical NiTi wire (table S1). This twistocaloric cooling was stable over 1000 cycles of twisting and untwisting up to 0.6 turns/cm (fig. S38). XRD results demonstrate reversible austenite-to-martensite conversion during twisting and untwisting a NiTi wire (Fig. 4B). Because this conversion is incomplete, there is an opportunity to increase twist-induced cooling by optimizing the NiTi composition and the operating temperature range of the cooler.

The calculated time for internal thermal equilibration of a 0.7-mm-diameter NiTi wire was 2.5 ms (18), which is much faster than the untwist process at 15 turns/s (65 to 455 ms). In agreement, the optically measured surface-average cooling upon untwisting a NiTi wire is close to the volume-average cooling (Fig. 4C) derived from the calorimetric specific cooling energy of this wire (18) (fig. S45). The anomalous behavior at very high twist, where cooling slightly decreases, is likely due to the onset of wire buckling. The maximum specific cooling energy (7.9 J/g) for untwisting the NiTi wire (Fig. 4C) is similar to literature results for stretch-released NiTi wires and sheets (5.0 to 9.4 J/g) and for stretch release of the present wires (9.4 J/g) (18).

A device that enabled one cycle of refrigeration was demonstrated for the cooling of a stream of water (Fig. 4D and figs. S46 and S47). Flowing ambient-temperature water over a three-ply NiTi wire cable, while removing 0.87 turns/cm of plying, cooled the water by

up to −4.7°C; higher water cooling (−7.7°C) resulted from adding thermal insulation, increasing the water channel diameter, and increasing the water flow rate (*18*). Integrating the cooling until the water stream returned to ambient temperature provided a specific cooling energy of 6.75 J/g (table S3), indicating that much of the cooling energy of the NiTi wire has effectively chilled the water. The twist-produced temperature changes of a thermochromic paint–coated NiTi wire provided visible indication of torsional rotation (fig. S34B and movie S4).

Summary

Twist release from fibers or fiber plies resulted in high cooling for materials as different as NR and NiTi. The material cooling efficiency was doubled (to 65%) and cooler length was reduced by a factor of two-sevenths by replacing elastocaloric cooling by twistocaloric cooling for NR fibers. A NiTi-based twist-fridge cooled flowing water by up to −7.7°C in one cycle.

Twist induced by stretch release from coiled polyethylene fishing line resulted in surface cooling that was more than 50 times higher than that obtained by releasing stretching from the nontwisted fiber. Depending on the relative chiralities of fiber and coil, polymers were engineered to cool either during stretch or stretch release. The spatial periodicity of surface temperature changes of coiled fibers can be an asset for remotely readable tensile and torsional strain sensors and for color-changing fibers for fabrics that dynamically respond to body movement.

REFERENCES AND NOTES

1. J. Gough, *Mem. Lit. Phil. Soc. Manchester 1 (2nd Series)* **288**, 288–295 (1805).
2. R. Ma *et al.*, *Science* **357**, 1130–1134 (2017).
3. B. Neese *et al.*, *Science* **321**, 821–823 (2008).
4. E. Defay *et al.*, *Nat. Commun.* **9**, 1827 (2018).
5. M. Trček *et al.*, *Philos. Trans. R. Soc. London Ser. A* **374**, 20150301 (2016).
6. X. Moya, S. Kar-Narayan, N. D. Mathur, *Nat. Mater.* **13**, 439–450 (2014).
7. T. Gottschall *et al.*, *Nat. Mater.* **17**, 929–934 (2018).
8. A. Chauhan, S. Patel, R. Vaish, C. R. Bowen, *MRS Energy Sustain.* **2**, E16 (2015).
9. J. Cui *et al.*, *Appl. Phys. Lett.* **101**, 073904 (2012).
10. J. Tušek, K. Engelbrecht, L. P. Mikkelsen, N. Pryds, *J. Appl. Phys.* **117**, 124901 (2015).
11. J. Tušek *et al.*, *Nat. Energy* **1**, 16134 (2016).
12. Y. Liu *et al.*, *Adv. Mater.* **26**, 6132–6137 (2014).
13. Y. Li *et al.*, *ACS Appl. Mater. Interfaces* **10**, 25438–25445 (2018).
14. S. Qian *et al.*, *Philos. Trans. R. Soc. London Ser. A* **374**, 20150309 (2016).
15. Y. Yoshida, K. Yuse, D. Guyomar, J. F. Capsal, G. Sebald, *Appl. Phys. Lett.* **108**, 242904 (2016).
16. I. Takeuchi, K. Sandeman, *Phys. Today* **68**, 48–54 (2015).
17. A. M. G. Carvalho, W. Imamura, E. O. Usuda, N. M. Bom, *Eur. Polym. J.* **99**, 212–221 (2018).
18. Materials and methods are available as supplementary materials.
19. T. L. Bergman, F. P. Incropera, D. P. DeWitt, A. S. Lavine, *Fundamentals of Heat and Mass Transfer* (Wiley, ed. 7, 2011).
20. S. L. Dart, R. L. Anthony, E. Guth, *Ind. Eng. Chem.* **34**, 1340–1342 (1942).
21. C. S. Haines *et al.*, *Science* **343**, 868–872 (2014).
22. Z. Xie, G. Sebald, D. Guyomar, *Phys. Lett. A* **381**, 2112–2116 (2017).
23. R. J. Young, P. B. Bowden, *Philos. Mag.* **29**, 1061–1073 (1974).
24. P. A. T. Olsson *et al.*, *Phys. Rev. Mater.* **2**, 075602 (2018).
25. R. Androsch, M. L. Di Lorenzo, C. Schick, B. Wunderlich, *Polymer* **51**, 4639–4662 (2010).
26. H. Tadokoro, *Polymer* **25**, 147–164 (1984).
27. Y. Jin, B. Wunderlich, *J. Phys. Chem.* **95**, 9000–9007 (1991).

Science

Torsional refrigeration by twisted, coiled, and supercoiled fibers

Run Wang, Shaoli Fang, Yicheng Xiao, Enlai Gao, Nan Jiang, Yaowang Li, Linlin Mou, Yanan Shen, Wubin Zhao, Sitong Li, Alexandre F. Fonseca, Douglas S. Galvão, Mengmeng Chen, Wenqian He, Kaiqing Yu, Hongbing Lu, Xuemin Wang, Dong Qian, Ali E. Aliev, Na Li, Carter S. Haines, Zhongsheng Liu, Jiuke Mu, Zhong Wang, Shougen Yin, Márcio D. Lima, Baigang An, Xiang Zhou, Zunfeng Liu and Ray H. Baughman

Twisting is cool

Rubber bands that are stretched and held in an extended shape for a while will extract heat from their surroundings as they are allowed to relax, owing to a reversal of stress-induced crystallization, which is an exothermic process. Wang *et al.* examine the potential for solid-state cooling of twisted fibers, along with configurations such as supercoiling, for materials including natural rubber, polyethylene, and nickel-titanium fibers. The cooling is related to the change in entropy of the material as it is mechanically deformed.

Science, this issue p. 216

ARTICLE TOOLS	http://science.sciencemag.org/content/366/6462/216
SUPPLEMENTARY MATERIALS	http://science.sciencemag.org/content/suppl/2019/10/09/366.6462.216.DC1
REFERENCES	This article cites 40 articles, 3 of which you can access for free http://science.sciencemag.org/content/366/6462/216#BIBL
PERMISSIONS	http://www.sciencemag.org/help/reprints-and-permissions

Use of this article is subject to the Terms of Service